ELSEVIER

Physica B 276–278 (2000) 17–21

PHYSICA B

www.elsevier.com/locate/physb

Neutron reflectometry on magnetic thin films

Hartmut Zabel[a,*], Ralf Siebrecht[b], Andreas Schreyer

[a]*Institut für Festkörperphysik, Ruhr-Universität Bochum, D-44780 Bochum, Germany*
[b]*Institute Laue-Langevin, F-38042 Grenoble Cedex, France*

Abstract

The current interest in the magnetism of ultrathin films is driven by their manifold applications in the nano-technology area, for instance as magnetic field sensors or as devices for information storage. Neutron scattering has played a dominant role for the determination of spin structures, phase transitions, and magnetic excitations in bulk materials. Today, its potential for the investigation of thin magnetic films has to be redefined. In the field of thin film magnetism, polarized neutron reflectivity (PNR) at small wave vectors can provide precise information on magnetization vectors in the film plane and on their variation from plane to plane. Therefore, neutron scattering remains the only method which allows to unravel the magnetization in thin films and superlattices independent of their thickness and depth below the surface. In addition, PNR is not only sensitive to structural interface roughness but also to the magnetic roughness. Some new developments will be discussed.

Keywords: Reflectometry; Polarised neutrons; Thin films; Planar ferromagnets

1. Introduction

The reflection of neutrons off planar surfaces dates back to the mid 1940s for determining the sign of the average coherent scattering length, and later in the 1960s for guidance of cold neutrons to instruments at far distance from the source. In the early 1980s neutron reflection was re-invented by Felcher as a powerful tool for specific condensed matter and materials science problems, in particular for the investigation of polymer, magnetic, and superconducting films [1]. Since then, the application of neutron reflectivity has seen a steady growth. The first wavelength dispersive neutron reflectometer with full polarization analysis was operating at the Frank Laboratory of Neutron Scattering in 1987, followed by an equivalent angle dispersive neutron reflectometer at the Research Reactor of the National Institute of Standards and Technology in 1992. An overview of the presently available instruments is provided in Ref. [2]. Only a few remarks on the method of polarized neutron reflectivity (PNR) shall be provided here. For further details the reader is referred to a number of reviews published during the last years [3–6].

2. Remarks to the method

Let us assume that a sample with a flat surface is in a ferromagnetic, single domain state and that the average magnetization vector of the sample makes an angle θ against the X-axis, as indicated in Fig. 1(a). Furthermore, we assume that a monochromatic and polarized neutron beam with polarization axis along the Y-direction impinges onto the sample at a glancing angle ϕ. In the Z-direction the neutron kinetic energy experiences a potential step composed of a nuclear and magnetic part: $V_{\mathrm{tot}} = V_{\mathrm{n}} \pm V_{\mathrm{m}}$. This changes the effective scattering length $b_{\mathrm{eff}}(\theta) = b_{\mathrm{coh}} \pm p_{\mathrm{m}} \sin(\theta)$, and total reflection occurs for the critical scattering vector $\boldsymbol{Q}_c^{\pm} = \sqrt{16\pi N_{\mathrm{A}} b_{\mathrm{eff}}^{\pm}}\,\hat{z}$. The $\pm$ sign refers to the parallel or antiparallel alignment of the neutron magnetic moment

* Corresponding author. Tel.: + 49-234-700-3649; fax: + 49-234-709-4173.
E-mail address: hartmut.zabel@ruhr-uni-bochum.de (H. Zabel)

0921-4526/00/$ - see front matter
PII: S0921-4526(99)01469-6

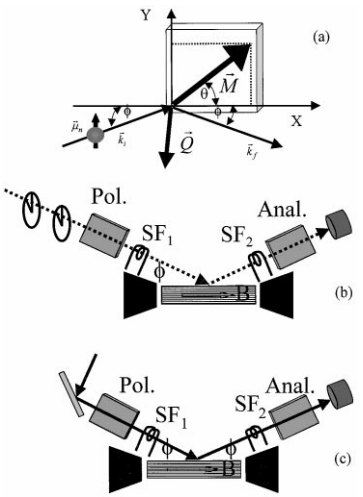

Fig. 1. (a) Scattering geometry for polarized neutron reflectivity studies. Y-refers is the quantization axis for the neutrons and the non-spin-flip axis, X is the spin-flips axis. (b) and (c) show schematic outlines of a wavelength and angle dispersive polarized neutron reflectometer, respectively.

with respect to the Y-axis, and p_m can be regarded as a magnetic scattering length. Thus any Y-component of a magnetic field distribution or a sample magnetization leads to two critical angles for total neutron reflection with respect to the two possible neutron spin polarizations. If the incident beam is unpolarized, for scattering vectors $\boldsymbol{Q}_c^- < \boldsymbol{Q} < \boldsymbol{Q}_c^+$, one polarized beam is reflected and the other one with the opposite polarization is refracted. This property is exploited in supermirrors for polarizing neutron beams, where either the reflected or the transmitted beam is being used for reflectivity measurements. The Y-axis is referred to as the non-spin -flip (NSF)-axis. The X-component of the magnetization vector, though not changing the refractive index, causes a perturbation of the neutron polarization, which over some optical path length flips the neutron spin from the $(+)$ to the $(-)$ state or vice versa. The spin-flip (SF) process is of purely magnetic origin and does not occur in coherent nuclear scattering. The respective $(+,-)$ and $(-,+)$ cross sections are always degenerate for the scattering geometry depicted in Fig. 1(a). From measuring the NSF and SF intensities the angle θ can be determined. In a stratified medium a potential step occurs at each interface and the scattering length along the sample normal becomes a function of the depth below the surface: $b_{\mathrm{eff}}(z,\theta) = b_{\mathrm{coh}}(z) \pm p_m(z)\sin(\theta)$. With polarized neutron reflectivity it is possible to measure the NSF reflectivities $R^{+,+}, R^{-,-}$ and the SF reflectivities $R^{+,-} = R^{-,+}$ and thus to retrieve the potential profile along the sample normal, including the nuclear density variation as well as the in-plane magnetization vector from layer to layer.

PNR studies are carried out either in a wavelength or in an angle dispersive mode, both are schematically depicted in Fig. 1(b) and (c). In both cases super-mirrors and spin-flippers are used in the incident and reflected beam. The super-mirror and spin-flipper can be integrated into one device if the remnant magnetization of the supermirror is high enough and if its magnetization can be switched from one orientation to the opposite with a pulsed field [7]. The main advantage of the wavelength dispersive mode is a fixed grazing angle to the sample surface. On the other hand, the angle dispersive mode has the advantage of a constant efficiency for the supermirrors and spin flippers, optimized for the particular wavelength used.

3. Magnetic heterostructure research with neutron scattering

In the past neutron scattering has contributed little to semiconductor physics and electronic devices. With the advent of magneto-electronic heterostructures in recent years, this situation has dramatically changed. Magneto-electronic heterostructures, in general, consist of ferromagnetic metal layers in conjunction with layers of paramagnetic metals, semiconductors, or antiferromagnetic insulators. Common features of magneto-electronic devices are the spin transport, the spin scattering, or the spin freezing of polarized electrons in defined orientations. They are used for nanoscale magnetic sensors and for non-volatile information storage devices. Magnetic structure information of these materials is very much needed from neutron scattering for their basic understanding and for further developments. The following provides a few examples.

3.1. Exchange coupled superlattices

Exchange coupled multilayers are important heterostructures for the study and application of the giant magneto-resistance effect. Fe/Cr superlattices are the archetypal system in this regard, for which an oscillatory RKKY-type exchange coupling was first discerned, including short and long period oscillations, collinear and non-collinear magnetic coupling angles between adjacent Fe layers, and a very large giant magneto-resistance (GMR) effect (for a review see e.g. Ref. [8]). Yet, the magnetic state of Cr and its role for the exchange coupling was not known until recently. For an ideally flat Fe/Cr interface and a Cr spacer thicker than required for half a period of the spin-density wave (SDW), we expect the antinode of the SDW to be placed next to the interface. Then the antiferromagnetic Fe–Cr interface coupling should be strong and the phase information controlling parallel or antiparallel alignment of successive Fe layers should be transmitted through the Cr

spacer. With increasing roughness, the Fe–Cr interface coupling becomes frustrated and a node of the SDW at the interface is energetically more favorable. A node however, weakens the Fe–Cr interface coupling and destroys the phase information. This scenario has indeed been observed in neutron scattering experiments on Fe/Cr superlattices by comparing interlayer exchange coupling with SDW order [9,10]. While at low temperatures a transverse incommensurate (I) - SDW exists with the ordering wave vector $\boldsymbol{Q}_{\mathrm{SDW}}$ normal to the film plane, the I-SDW order vanishes by passing a transition region above the Néel temperature and is replaced by a commensurate (C)-SDW. The C-SDW phase exhibits a much higher Néel temperature than the I-SDW phase, the former depending on the proximity to the Fe layer and the latter on the scaling with thickness. These experiments also revealed that in the low-temperature I-SDW phase the exchange coupling is very weak, whereas in the high-temperature C-SDW phase the Cr spin structure mediates a strong non-collinear exchange coupling. In Fig. 2 neutron scattering data are reproduced for a Fe/Cr superlattice with a Cr thickness of 42 Å. The low-angle reflectivity measurements reveal a non-collinearly coupled superlattice, while the high-angle data confirm a commensurate Cr spin structure. In addition, the superlattice periodicity is imprinted not only on the structure factor of the Fe layers but also on the Cr layers. Thus both, the ferromagnetic and antiferromagnetic layers are modulated by the same superlattice periodicity. According to the proximity exchange model introduced by Slonczewski [11], lateral thickness fluctuations of monoatomic high steps require the Cr spin structure to be twisted counterclockwise on either side of a step in order

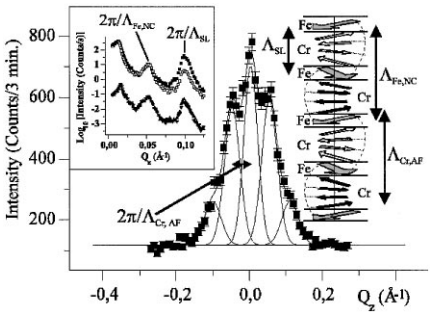

Fig. 2. Neutron scattering from a Fe/Cr superlattice with a Cr spacer thickness of 42 Å. In the center is shown a scan at the (0 1 0) Bragg position in the z-direction, revealing a commensurate Cr(0 1 0) peak modulated by the magnetic superlattice periodicity. The inset in the upper left corner shows polarized neutron reflectivity data, revealing a non-collinear arrangement of the Fe layer magnetization vectors. In the upper right inset is sketched the most reasonable spin structure in the Fe/Cr superlattice with respect to the experimentally determined boundary conditions.

to couple to a homogeneous Fe layer magnetization. The neutron scattering results corroborate this model and thus provide the missing link between SDW order in thin Cr films as a function of temperature and thickness, the coupling strength, and the orientation of the Fe magnetization vectors [9,10,12]. The shape of the GMR effect depends sensitively on these properties and can now be calculated in detail [13].

3.2. Exchange bias

The exchange coupling between thin itinerant ferromagnetic layers (F) and antiferromagnetic substrates (AF) leads to an unusual asymmetry of the magnetic hysteresis M(H) [14]. In fact, the exchange anisotropy for F/AF heterostructures is a unidirectional anisotropy giving rise to one easy axis of magnetization. Although discovered more than 50 years ago, it is not until recently that this effect has gained tremendous technological importance in spin-valve systems for magnetic field sensors and for the stabilization of magnetic domains in magneto-resistive reading heads. The exchange bias has been observed for F/AF layers in direct contact, as well as in indirect contact across a diamagnetic interlayer. In most cases the AF layer is an antiferromagnetic insulator. However, most recently an exchange bias effect has also been observed for a completely metallic system [15]. Using a double Fe/Cr superlattice, consisting of a ferromagnetically coupled Fe/Cr superlattice grown on top of an antiferromagnetically coupled Fe/Cr superlattice, both coupled antiferromagnetically via a Cr spacer in between, a hysteresis with a clear exchange field can be observed after field cooling. Subsequently neutron reflectivity measurements were taken at two specific points along the hysteresis loop just before magnetization reversal along the descending field and on the ascending field branch. The neutron reflectivity results in terms of the neutron spin asymmetry $P = (R_+ - R_-)/(R_+ - R_-)$ reveals significant differences for both magnetization branches, indicative for different spin structures at the F/AF interface. The microscopic origin of the bias exchange is not completely clear up to now. Usually it is assumed that the interface exchange coupling between the F and AF layer breaks the symmetry upon favoring one of the AF sublattices by the orientation of the external field during field cooling of the system below the Néel temperature of the AF layer. In the simplest case these models assume a layered antiferromagnetic structure close to the interface (fully uncompensated). Recent experiments, however, show that this notion is too simple. Exchange bias also occurs if the interface is magnetically compensated [16,17]. Then a 90°-coupling between the magnetic moments of the F and AF layer appears typically. This is confirmed by molecular field-type calculations, indicating a spin-flop mechanism due to frustrated bilinear interface coupling. If domain walls

occur along the interface, interface roughness should reduce the exchange bias effect, which, however, is contrary to observations [18]. All experiments so far have concentrated on the magnetic hysteresis of the F layer, since there is no easy way to determine the domain structure of the AF layer. Neutron scattering is indeed the only method to reveal the antiferromagnetic structure of materials and to shed light on the domain wall separation.

3.3. Magnetic roughness

It is readily appreciated that magnetic roughness plays an important role for the performance of magnetoelectronic devices. The GMR amplitude, the exchange coupling strength and the exchange field are examples for properties which depend strongly on the interface roughness. Obviously the magnetic and structural roughness may not be the same. Interdiffusion may cause spin canting, spin glass properties or a complete quenching of the magnetic moments, as is the case at Fe/Nb interfaces [19]. The structural roughness is often characterized by a height–height correlation function for a self-affine and fractal surface [20]: $C(R) = \langle z(0)z(R)\rangle = \sigma^2 \exp[-(R/\xi)]^{2h}$, where $z(0)$ and $z(R)$ is the height above an average surface at the origin and at the distance R, respectively, σ is the mean square roughness, ξ is the cut-off length, and h is the Hurst parameter, describing the jaggedness of the interface. The structural roughness gives rise to diffuse off-specular scattering in X-ray and neutron reflectivity scans. The description of magnetic roughness and its interpretation is far more difficult and still in its infancy [21]. On the one hand, the magnetic roughness must be smoother than the structural roughness because of the magnetic permeability of most materials, allowing the magnetic field lines to penetrate through hills and valleys. On the other, a single step at an Fe/Cr interface being a negligible structural defect, may cause a complete reorientation of the SDW with much spin canting close to the interface [22]. Magnetic roughness must eventually decay either in a high enough magnetic field or above the Curie temperature. Off-specular polarized neutron reflectivity is particular suitable for analyzing magnetic roughness. First, the SP cross section allows a separation between magnetic and structural contributions, and second the field or temperature dependence are sensitive indicators for the presence of magnetic roughness.

In Fig. 3 are shown transverse scans of an antiferromagnetically coupled Fe/Cr superlattice. The scans are taken across the half order peak at the position $K = \pi/\Lambda$ with different cross sections, where Λ is the superlattice periodicity. The $(+,+)$ cross section is independent of the magnetic field, whereas the $(-,-)$ cross section is sensitive to the progressively increasing ferromagnetic order with increasing external magnetic field. Thus the

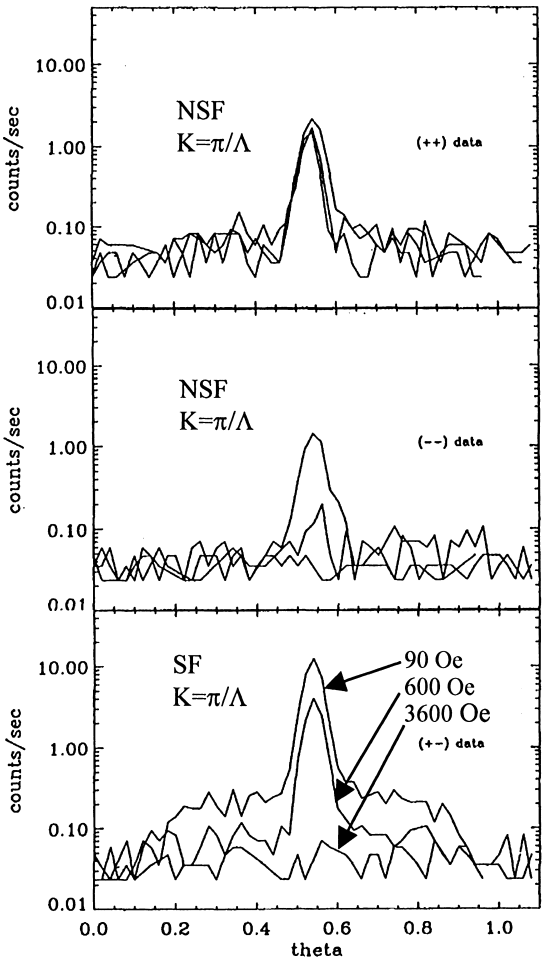

Fig. 3. Transverse scans taken across the half order antiferromagnetic peak of an antiferromagnetically coupled Fe/Cr superlattice as a function of external field. The scans are taken with different cross sections. The top and middle panel reproduce the non-spin-flip (NSF) scattering results, the bottom panel shows the spin flip (SF) measurements.

intensity of this peak decreases with increasing field. Both transverse scans do not exhibit much diffuse scattering away from the specular ridge, indicating that the structural roughness is minimal. This is also confirmed by x-ray scattering experiments on the same sample. It is only in the SP $(+,-)$ and $(-,+)$ cross sections that diffuse scattering can be recognized. This diffuse scattering strongly depends on the field strength, proving that it is of magnetic origin, whereas the structural roughness does not depend on the magnetic field. At this point we should recall that the polarized neutron reflectivity is sensitive to the magnetic induction and not to the local magnetic moments. Therefore, with increasing field it is

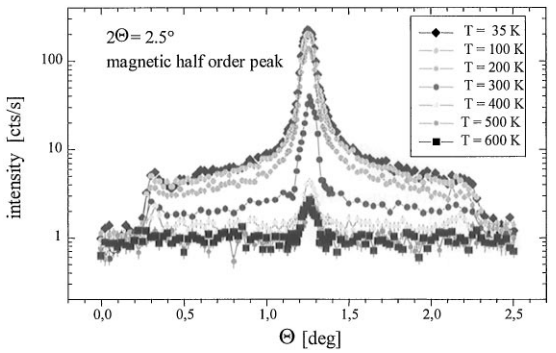

Fig. 4. Off-specular diffuse polarized neutron scattering from a $Fe_{0.43}Cr_{0.57}$/Cr superlattice. The data are taken at the half-order antiferromagnetic peak. The strong diffuse scattering occurs only below the Curie temperature of about 450 K.

natural to assume that the field lines become more straight, reflecting a magnetically smoother interface. Determination of spin disorder on an atomic scale would require scans at higher scattering vectors.

In Fig. 4 off-specular diffuse scans are shown as a function of temperature, which were taken at the antiferromagnetic π/Λ position of an antiferromagnetically coupled $Fe_{1-x}Cr_x/Cr(x = 0.57)$ superlattice. In this case, a ferromagnetic alloy layer was used to reduce the Curie-temperature below the temperature where interdiffusion starts to take place. At low temperatures the diffuse scattering is strong due to a magnetically rough interface causing magnetic frustrations in the exchange coupled superlattice. With increasing temperature the diffuse scattering diminishes and above the Curie temperature a weak sharp peak is visible from the specular ridge. The specular peak is due to the structural interface, which has not changed upon heating. This indicates that the structural roughness is much lower than the magnetic one.

4. Conclusions

The analysis and understanding of new magneto-electronic heterostructures is an important field with much potential for neutron scattering research in the future. Only a few examples could be discussed here. Not mentioned have been ferromagnetic/superconducting interfaces with proximity effects, spring magnets consisting of alternating soft and hard magnetic layers, and laterally structured magnetic systems. The magnetic roughness at interfaces needs to be better characterized and understood in the future. For the performance of spinelectronic devices it is presently not clear whether disorder of local moments or of the magnetic field distribution is the more important parameter. It must also be tested to what extend spin-flip of neutrons yields information on the spin flip of electrons in these magnetic heterostructures. Scattering experiments with neutrons and with synchrotron radiation will continue to prove most useful in this context.

This work was supported by the Bundesministerium für Bildung und Forschung under contract 03-ZA5BC20 and the Landesministerium NRW für Wissenschaft und Forschung.

References

[1] G.P. Felcher, Phys. Rev. B 24 (1981) 1595.
[2] G.P. Felcher, Physica B 267–268 (1999) 154.
[3] C.F. Majkrazak, Physica B 213 (1995) 904.
[4] C.F. Majkrazak, Physica B 221 (1996) 342.
[5] G.P. Felcher, Physica B 192 (1993) 137.
[6] A. Schreyer, J. Phys. Soc. Japan 65 (Suppl. A 1) (1996) 13.
[7] P. Böni et al., Physica B 267 (1999) 320.
[8] B. Dieny, J. Magn. Magn. Mater. 136 (1994) 335.
[9] A. Schreyer et al., Phys. Rev. Lett. 79 (1997) 4914.
[10] A. Schreyer et al., J. Magn. Magn. Mater. (2000) accepted.
[11] J.C. Slonczewski, J. Magn. Magn. Mater. 150 (1995) 13.
[12] E.E. Fullerton, S.D. Bader, J.L. Robertson, Phys. Rev. Lett. 77 (1996) 1382.
[13] V.V. Ustinov et al., Phys. Rev. B 54 (1996) 15958.
[14] J. Nogués, I.K. Schuller, J. Magn. Magn. Mater. 192 (1999) 203.
[15] J.S. Jiang, G.P. Felcher, A. Inomata, R. Goyette, C. Nelson, S.D. Bader, preprint.
[16] J. Nogués et al., Phys. Rev. Lett. 76 (1996) 4624.
[17] J. Nogués et al., Phys. Rev. B 59 (1999) 6984.
[18] Y. Ijiri et al., Phys. Rev. Lett 80 (1998) 608.
[19] Th. Mühge et al., Phys. Rev. B 55 (1977) 8945.
[20] S.K. Sinha, E.B. Sirota, S. Garoff, H.B. Stanley, Phys. Rev. B 38 (1988) 2297.
[21] B.P.Toperverg et al., in these Proceedings (ECN '99), Physica B 276–278 (2000).
[22] P. Bödeker et al., Phys. Rev. Lett. 81 (1998) 914.